

AD_____

Award Number: W81XWH-10-1-0275

TITLE: Androgenic Regulation of White Adipose Tissue-Prostate Cancer Interactions

PRINCIPAL INVESTIGATOR: Timothy C. Thompson, Ph.D.

CONTRACTING ORGANIZATION: University of Texas MD Anderson Cancer Center
Houston, TX 77030

REPORT DATE: May 2012

TYPE OF REPORT: Annual

PREPARED FOR: U.S. Army Medical Research and Materiel Command
Fort Detrick, Maryland 21702-5012

DISTRIBUTION STATEMENT: Approved for Public Release;
Distribution Unlimited

The views, opinions and/or findings contained in this report are those of the author(s) and should not be construed as an official Department of the Army position, policy or decision unless so designated by other documentation.

REPORT DOCUMENTATION PAGE				<i>Form Approved</i> OMB No. 0704-0188	
Public reporting burden for this collection of information is estimated to average 1 hour per response, including the time for reviewing instructions, searching existing data sources, gathering and maintaining the data needed, and completing and reviewing this collection of information. Send comments regarding this burden estimate or any other aspect of this collection of information, including suggestions for reducing this burden to Department of Defense, Washington Headquarters Services, Directorate for Information Operations and Reports (0704-0188), 1215 Jefferson Davis Highway, Suite 1204, Arlington, VA 22202-4302. Respondents should be aware that notwithstanding any other provision of law, no person shall be subject to any penalty for failing to comply with a collection of information if it does not display a currently valid OMB control number. PLEASE DO NOT RETURN YOUR FORM TO THE ABOVE ADDRESS.					
1. REPORT DATE May 2012		2. REPORT TYPE Annual		3. DATES COVERED 1 May 2011 – 30 April 2012	
4. TITLE AND SUBTITLE Androgenic Regulation of White Adipose Tissue-Prostate Cancer Interactions				5a. CONTRACT NUMBER	
				5b. GRANT NUMBER W81XWH-10-1-0275	
				5c. PROGRAM ELEMENT NUMBER	
6. AUTHOR(S) Timothy C. Thompson, Ph.D. E-Mail: timthomp@mdanderson.org				5d. PROJECT NUMBER	
				5e. TASK NUMBER	
				5f. WORK UNIT NUMBER	
7. PERFORMING ORGANIZATION NAME(S) AND ADDRESS(ES) University of Texas MD Anderson Cancer Center Houston, TX 77030				8. PERFORMING ORGANIZATION REPORT NUMBER	
9. SPONSORING / MONITORING AGENCY NAME(S) AND ADDRESS(ES) U.S. Army Medical Research and Materiel Command Fort Detrick, Maryland 21702-5012				10. SPONSOR/MONITOR'S ACRONYM(S)	
				11. SPONSOR/MONITOR'S REPORT NUMBER(S)	
12. DISTRIBUTION / AVAILABILITY STATEMENT Approved for Public Release; Distribution Unlimited					
13. SUPPLEMENTARY NOTES					
14. ABSTRACT Adipocyte stromal cells from WAT of both Glipr1 wild type adult males and Glipr1 knock out adult males were isolated and used for coculturing experiment. Coculturing prostate cancer cells (VCaP, RM-9, PC-3) with ASCs from WAT of Glipr1 KO and Glipr1 WT resulted in increased growth of the cancer cells compared to the cells grown without the ASCs. Moreover, the prostate cancer cells grown with Glipr1 KO ASCs resulted in higher cell growth rate compared to the cells grown with Glipr1 WT ASCs. Similar results were found after the prostate cancer cells were incubated with ASCs-CM from both Glipr1 KO and WT. The cells incubated with Glipr1 KO ASCs-CM resulted in higher cell growth number compared to the cells grown with Glipr1 WT ASCs-CM, indicating the presence of differential levels of factors that promote cell growth. When the ASCs-CM from Glipr1 WT and KO were analyzed and compared, we detected numerous factors that promote tumor cell growth and invasion. As expected, the levels of these factors that promote cancer cell growth and invasion were much higher in Glipr1 KO ASCs-CM than in Glipr1 WT ASCs-CM.					
15. SUBJECT TERMS Prostate cancer					
16. SECURITY CLASSIFICATION OF:			17. LIMITATION OF ABSTRACT UU	18. NUMBER OF PAGES 23	19a. NAME OF RESPONSIBLE PERSON USAMRMC
a. REPORT U	b. ABSTRACT U	c. THIS PAGE U			19b. TELEPHONE NUMBER (include area code)

TABLE OF CONTENTS

Introduction.....	4
Body.....	5
Key Research Accomplishments.....	9
Reportable Outcomes	10
Conclusion	11
References.....	12
Appendices.....	13

2012 PROGRESS REPORT

INTRODUCTION

Prostate cancer (PCa) cells are initially sensitive to hormonal manipulation, and androgen-deprivation therapy (ADT) generally reverses androgen receptor (AR)–dependent growth and proliferation. ADT is one of the main treatment modalities in the clinical management of PCa, but ADT is only palliative, and PCa eventually progresses to an androgen-insensitive stage, i.e., castrate-resistant PCa (CRPC), after a median of 12–20 months. Progression to CRPC is a dynamic process that is incompletely understood as yet. Potential mechanisms contributing to the development of CRPC include selective growth of a preexisting hormone-insensitive population of cancer cells as a result of suppression by androgen ablation of the androgen-dependent cell population; activation of oncogenes; inactivation of tumor suppression genes; and interaction between cancer cells and tumor-associated stroma and tumor-associated macrophages. The object of this research project is to investigate the effect of castration on epididymal white adipose tissue (WAT), ventral prostate (VP) tissue, and adipose stromal cells (ASCs) from male *Glipr1*^{+/+} wild-type (WT) and *Glipr1*^{-/-} knockout (KO) mice. We are testing our hypothesis that the biologic activity of WAT is affected by castration and that although the acute effects of castration (e.g., GLIPR1 induction) may suppress cancer-promoting adipokines, long-term ADT results in monocyte infiltration and the generation of WAT-associated macrophages (WAMs). WAMs, in turn, produce cytokines and promote the growth and survival of growth factor–expressing ASCs, which enter the systemic circulation and promote PCa progression. An important note is that the prostate, an androgen target organ, is significantly affected by castration and also produces cytokines and cytokine receptors that may, in concert with WAT-derived cytokines, contribute to the progression of already established local tumors. We also hypothesize that *Glipr1*/GLIPR1 protein regulates castration-induced WAMs and ASCs. Our overarching hypothesis is that castration induces alterations in WAT that promote the development of CRPC. During the second funding period, we have completed the studies proposed in Specific Aim 2.

Key Personnel

Principal Investigator: Timothy C. Thompson, Ph.D.; 713-792-9955; timthomp@mdanderson.org
Co-Investigator: Takahiro Hirayama, M.D.; 713-792-8932; thirayama@mdanderson.org
Co-Investigator: Guang Yang, M.D., Ph.D.; 713-563-9004; guangyang@mdanderson.org

BODY

STATEMENT OF WORK

Aim 1: Identify castration-affected and/or *Glipr1*-regulated genes in ventral prostate (VP) tissue, epididymal white adipose tissue (WAT), and adipocyte stromal cells (ASCs) using in vivo models.

1. Generate a sufficient number of *Glipr1* wild-type (WT) and *Glipr1* knockout (KO) 12-week-old male mice (1–6 months).
2. Perform the surgical castration experiment using the *Glipr1* WT and KO male mice, and collect VP, WAT, and ASCs on days 3, 14, and 35 after castration (6–9 months).
3. Isolate RNA and perform microarray analyses to characterize genes affected by castration in VP, WAT, and ASCs in *Glipr1* WT and KO male mice (9–12 months).

Aim 2: Study the interactions between ASCs isolated from *Glipr1* WT (ASCs-WT) and KO (ASCs-KO) male mice and human prostate cancer cell lines in vitro and in vivo.

1. Isolate, expand, and prepare a stock of frozen ASCs from *Glipr1* WT and KO male mice (6–12 months).
2. Determine the effect of ASCs on the cell growth rate of human prostate cancer cell lines in vitro (12–18 months).
3. Determine the effect of ASCs conditioned media on the cell growth rate of human prostate cancer cell lines in vitro (12–18 months).
4. Analyze and compare cytokine and growth factor profiles in conditioned media produced by ASCs (18–24 months).

RESEARCH

Materials and Methods

Isolation of stromal cells (ASC) from WAT

We enlarged the mice colony to generate enough males to isolate sufficient WAT pad for the proposed experiments since final number of ASC cells obtained were a small fraction of WAT pad harvested. WAT pads were collected from 12-week old male *Glipr1* WT and KO mice. The tissue was cut with scissors and digested with collagenase I for up to 60 min at 37°C. The digested tissue was then filtered through a 100- μ m filter. Next, the filtrate was centrifuged at 150 g for 5 min. The pellet was treated with erythrocyte lysis buffer and centrifuged again at 150 g for 5 min. The resulting cell pellet was resuspended in high-glucose DMEM with 10% fetal bovine serum, and the suspension was plated onto 10-cm culture plates.

Coculture Experiments

ASC: One mouse prostate cancer cell line, RM-9, and two human prostate cancer cell lines, VCaP and PC-3, were used for this coculture study. Regular DMEM, high glucose DMEM, and RPMI 1640 was used to grow RM-9, VCaP and PC-3 cells respectively. Each of the three cell lines were cocultured with ASCs from *Glipr1* WT and KO mice using 0.4 μ m pore size translucent PET membrane inserts (BD Falcon, Franklin Lakes, NJ) for this aim. For PC-3 cells and RM-9 cells, 5×10^3 cells each were plated with 1% FBS growth medium in 24 well plates and allowed to establish overnight. For VCaP cells, 1×10^4 cells were plated with 10% FBS growth medium. Next morning, cells from each cell lines were cocultured with 1×10^4 ASCs isolated from *Glipr1* WT and KO mice using the PET membrane.

After 72 hour incubation for PC-3, and 48 hour incubation for RM-9 and VCaP, the number of living cells was measured using an 3-(4,5-dimethylthiazol-2-yl)-5-(3-carboxymethoxyphenyl)-2-(4-sulfophenyl)-2H-tetrazolium (MTS) assay (Celltiter 96 Aqueous One-solution Cell Proliferation assay)(Promega, Madison, WI) according to the manufacturer's instructions. Absorbance at 490 nm was measured using a multiwell plate reader (Bio-Rad).

ASCs-CM

Both genotypes of ASCs (Gliplr1 WT and KO) conditioned medium (ASCs-CM) were collected after 24h of incubation at 37°C with serum free DMEM from a dish initially seeded with 1×10^6 of the ASCs. CM was collected, and centrifuged at 1000g for 30 min at 4°C, then stored in -80°C until use.

The same cell culture conditions described above were employed to study the effect of ASCs conditioned media on the cell growth rate of the three cell lines without the use of PET membrane inserts. However, all three cell lines were grown in 96-well plate with 0.5% FBS+ the growth medium. After the cells were well established overnight, mixture of 50 μ l of the growth medium and 50 μ l of each ASCs-CM (Gliplr1 WT and Gliplr1KO) were added to the cells. The growth rate of VCaP and RM-9 were measured after 48 hours of incubation, but 72 hours for PC-3.

Antibody array

We used a Label-based Mouse Antibody Array (Raybiotech, Inc, Norcross, GA) to detect cytokines or growth factors in ASCs- CM from both genotypes according to the manufacturer's instructions. The expression levels of the cytokines and the growth factors were calculated against the internal control embedded in the kit.

Statistical analysis

The statistical significance of the differences between the cell growth of Gliplr1 WT and KO ASCs on different cell lines was determined by using two-tailed Student's *t* testing. The level of significance was set at $P < 0.05$.

Data are expressed as means \pm SE.

RESULTS

ASCs, ASCs-CM coculture:

The rate of cell growth increased for VCaP, PC-3 and RM-9 cells after they were cocultured with either Gliplr1 WT or KO ASCs compared to the cells grown without the ASCs (Fig. 1). We found statistically significant growth advantage for the cells grown with Gliplr1 KO ASCs compared to Gliplr1 WT ASCs in all three prostate cell lines. Similar growth advantages were seen in the cells incubated with the mixture of the growth medium + ASCs-CMs (either from Gliplr1 WT and KO) over the cells grown without the ASCs-CM (Fig. 2). Again, the cells incubated with Gliplr1 KO ASCs-CM showed increased cell proliferation compare to the cells incubated with Gliplr1 WT ASCs-CM.

Fig. 1

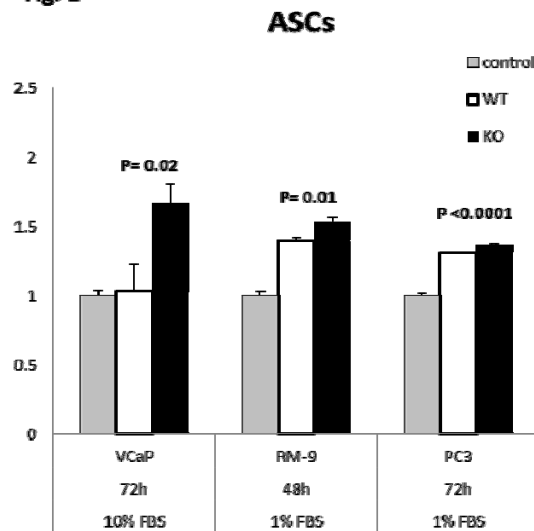


Fig. 1. Comparison of cell growth rate under the influence of ASCs. VCaP, PC-3 and RM-9 prostate cancer cell were cocultured either with Gliplr1 WT ASC(WT), Gliplr1 KO ASC (KO), and negative control (control). After 5×10^3 PC-3, 5×10^3 RM-9 and 1×10^4 VCaP cells were well established overnight, they were cocultured with either 1×10^6 Gliplr1 WT ASCs , 1×10^6 Gliplr1 KO ASCs, or without ASCs. After 72 hours for VCaP and PC-3, but 48 hours for RM-9, the cell growth was measured. The cell growth rate under different coculturing conditions were expressed compared to negative control (value=1) for each cell lines. P values indicate statistically significant growth differences between Gliplr1 WT ASCs and Gliplr1 KO ASCs.

As was proposed in this grant, these growth promoting factors in CM are secreted from ASC (both Glipr1 WT and KO).

Numerous factors promoting angiogenesis, tumor cell motility and metastasis were found ASCs-CMs of both Glipr1 WT and Glipr1 KO. But substantially higher levels of these factors were found in Glipr1 KO ASCs-CM than in Glipr1 WT ASCs-CM as shown in Fig.3. For example, although the relative signals of VE-cadherin is low, the level of VE-cadherin in Glipr1 KO ASCs-CM was 78 times higher than in Glipr1 WT ASCs-CM. VE-cadherin is an endothelial cell adhesion molecule and marker of tumor angiogenesis induction(1). Similarly, although CD11b level is relatively low compared to other factors, its expression level in Glipr1 KO ASCs-CM is 7.7 times higher than Glipr1 WT ASCs-CM. CD11b+ cells in bone marrow has been reported to be enriched for osteoclast precursors which cause bone resorption in prostate cancer metastasis(2). Further, CD11b+ cells has been shown to stimulate tumor endothelial cell cord formation by 10-fold in an in vitro angiogenesis assay (3). Chemokine receptor CCR9 in Glipr1 KO ASCs-CM expression level was 5.4 times higher than Glipr1 WT ASCs-CM. CCR9 with its natural ligand CCL25 has been shown to be highly expressed by prostate cancer cells (4). It has been shown to affect cancer cell migration, invasion, and MMP expression which together are involved in cancer cell metastasis (5, 7). Further, it is known to upregulate antiapoptotic proteins such as P13K, AKT, ERK1/2 and GSK-3 β (6).

Relatively high level of prolactin in the ASCs-CM is tantalizing, and may in part, explain increased cell growth observed in the prostate cancer cells incubated with ASCs-CM (from Glipr1 WT and KO) in Fig.2. Production of prolactin level has been shown to be increased in high grade prostate cancers (8), and has been shown to have tumorigenic roles through providing mitogenic and prosurvival effects.

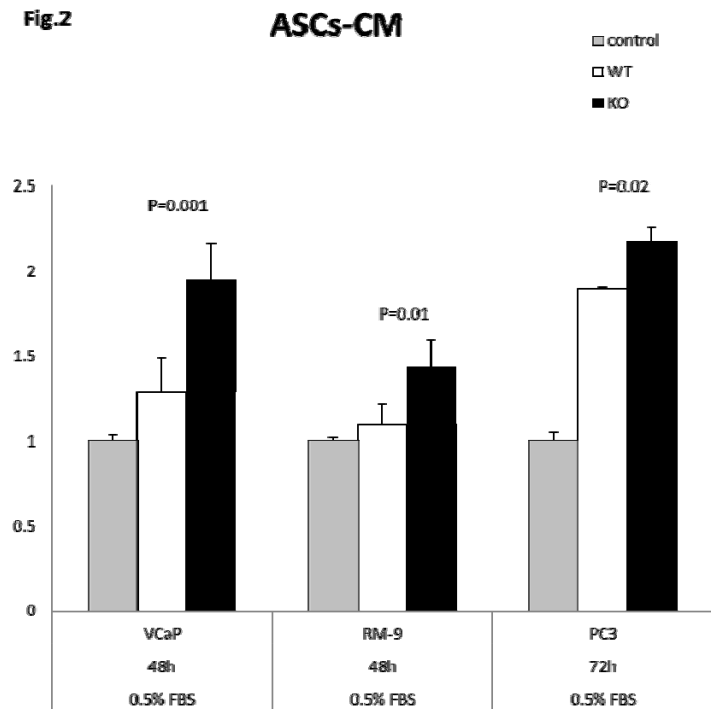


Fig. 2. Comparison of cell growth rate grown in the presence of ASCs-CM. VCaP, PC-3 and RM-9 prostate cancer cell were incubated with 1:1 mixture of the growth media and ASCs-CM (either from Glipr1 WT or Glipr1 KO), or without ASCs-CM. After 5×10^3 PC-3, 5×10^3 RM-9 and 1×10^4 VCaP cells were well established overnight, they were incubated with the mixture for 48 hours for VCaP and RM-9,. The difference in the cell growth rate was expressed and compared to the negative control value (value=1). However, the growth rate of PC-3 cells was measured after 72 hour incubation. P values indicate statistically significant growth differences between Glipr1 WT ASCs-CM and Glipr1 KO ASCs-CM.

Fig 3

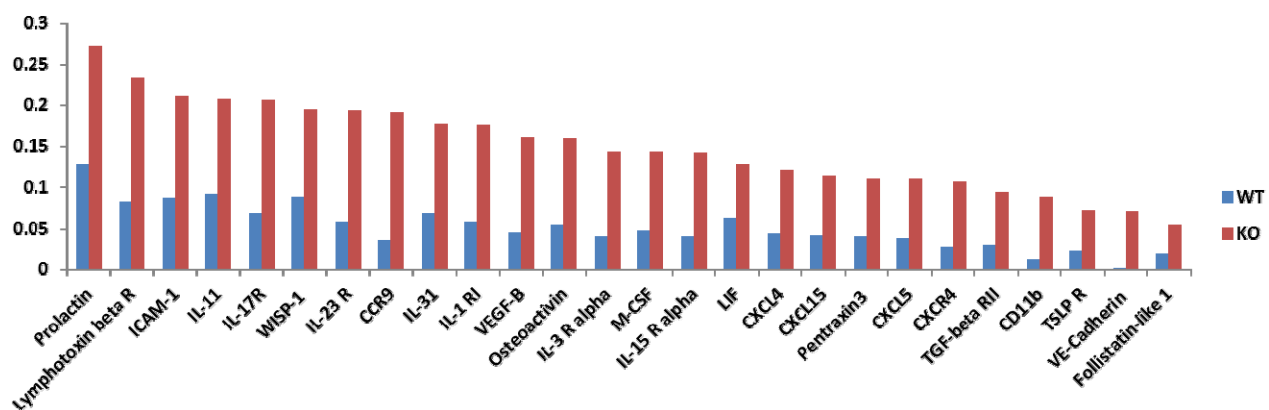


Fig. 3. Comparison of cytokine and growth factor levels in Glipr1 KO and WT ASCs-CM by antibody array. The expression level was normalized by the internal control embedded in the array kit.

KEY RESEARCH ACCOMPLISHMENTS

1. ASCs isolated from WAT of adult Glipr1 WT and KO males provided advantageous condition to prostate cancer cell (VCaP, RM-9, PC-3) growth when cocultured.
2. Coculturing the prostate cancer cells with ASCs from Glipr1 KO resulted in significantly higher cell proliferation than Glipr1 WT.
3. Incubating prostate cancer cells with CM from ASCs of Glipr1 WT and KO resulted in increased cell proliferation compared to the negative control.
4. Incubation with Glipr1 KO ASCs-CM resulted in higher prostate cancer cell growth rate than incubation with Glipr1 WT ASCs-CM.
5. Antibody array study detected numerous factors that promote cancer cell growth and invasion in ASCs-CMs. Glipr1 KO ASCs-CM contained much higher concentration of these factors that induce cancer cell growth and invasion than Glior1 WT ASCs-CM.

REPORTABLE OUTCOMES

1. Floryk D, Kurosaka S, Tanimoto R, Yang G, Goltsov A, Park S, Thompson TC. Castration-induced changes in mouse epididymal white adipose tissue. *Mol Cell Endocrinology* 2011, Oct 15: 345(1-2): 58-67.

CONCLUSIONS

Coculturing prostate cancer cells with ASCs from WAT of Glipr1 KO and Glipr1 WT resulted in increased cancer cell growth compared to the cancer cells grown without the ASCs. Moreover, the prostate cancer cells grown with Glipr1 KO ASCs resulted in higher cell growth compared to the cells grown with Glipr1 WT ASCs. Similar results were found after the prostate cancer cells were incubated with ASCs-CM from both Glipr1 KO and WT. The cells incubated with Glipr1 KO ASCs-CM resulted in higher cell growth compared to the cells grown with Glipr1 WT ASCs-CM. These results indicated presence of factors that promote cell growth in the ASCs-CMs. When the ASCs-CM from Glipr1 WT and KO were analyzed and compared by antibody array, we detected numerous factors that promote tumor cell growth and invasion. As expected, the levels of these factors that promote cancer cell growth and invasion were much higher in Glipr1 KO ASCs-CM than in Glipr1 WT ASCs-CM.

REFERENCES

1. Shih SC, Robinson GS, Perruzzi CA, Calvo A, Desai K, Green JE, Ali IU, Smith LE, Senger DR. Molecular profiling of angiogenesis markers. *Am J Pathol* 161(1):35-41, 2002.
2. Mizutani K, Sud S, Pienta KJ. Prostate cancer promotes CD11b positive cells to differentiate into osteoclasts. *J Cell Biochem* 106(4):563-9, 2009.
3. Dudley AC, Udagawa T, Melero-Martin JM, Shih SC, Curatolo A, Moses MA, Klagsbrun M. Bone marrow is a reservoir for proangiogenic myelomonocytic cells but not endothelial cells in spontaneous tumors. *Blood* 116(17):3367-71, 2010. Epub 2010 May 7.
4. Singh S, Singh UP, Stiles JK, Grizzle WE, Lillard JW Jr. Expression and functional role of CCR9 in prostate cancer cell migration and invasion. *Clin Cancer Res* 10(24):8743-50, 2004.
5. Johnson-Holiday C, Singh R, Johnson E, Singh S, Stockard CR, Grizzle WE, Lillard JW Jr. CCL25 mediates migration, invasion and matrix metalloproteinase expression by breast cancer cells in a CCR9-dependent fashion. *Int J Oncol* 38(5):1279-85, 2011. doi: 10.3892/ijo.2011.953. Epub 2011 Feb 23.
6. Sharma PK, Singh R, Novakovic KR, Eaton JW, Grizzle WE, Singh S. CCR9 mediates PI3K/AKT-dependent antiapoptotic signals in prostate cancer cells and inhibition of CCR9-CCL25 interaction enhances the cytotoxic effects of etoposide. *Int J Cancer* 127(9):2020-30, 2010.
7. Singh R, Stockard CR, Grizzle WE, Lillard JW Jr, Singh S. Expression and histopathological correlation of CCR9 and CCL25 in ovarian cancer. *Int J Oncol* 39(2):373-81, 2011. doi: 10.3892/ijo.2011.1059. Epub 2011 May 31.
8. Rouet V, Bogorad RL, Kayser C, Kessal K, Genestie C, Bardier A, Grattan DR, Kelder B, Kopchick JJ, Kelly PA, Goffin V. Local prolactin is a target to prevent expansion of basal/stem cells in prostate tumors. *Proc Natl Acad Sci U S A* 107(34):15199-204, 2010. Epub 2010 Aug 9.
9. Varghese B, Swaminathan G, Plotnikov A, Tzimas C, Yang N, Rui H, Fuchs SY. Prolactin inhibits activity of pyruvate kinase M2 to stimulate cell proliferation. *Mol Endocrinol* 24(12):2356-65, 2010. Epub 2010 Oct 20.

APPENDICES

1. Floryk D, Kurosaka S, Tanimoto R, Yang G, Goltsov A, Park S, Thompson TC. Castration-induced changes in mouse epididymal white adipose tissue. *Mol Cell Endocrinology* 345(1-2): 58-67, 2011.



Castration-induced changes in mouse epididymal white adipose tissue

Daniel Floryk, Shinji Kurosaka, Ryuta Tanimoto, Guang Yang, Alexei Goltsov, Sanghee Park, Timothy C. Thompson*

Department of Genitourinary Medical Oncology – Research, The University of Texas MD Anderson Cancer Center, Houston, TX, USA

ARTICLE INFO

Article history:

Received 2 June 2011

Accepted 5 July 2011

Available online 12 July 2011

Keywords:

Castration

Regular diet

High-fat diet

Epididymal white adipose tissue

C57BL/6J mouse

ABSTRACT

We analyzed the effects of castration on epididymal white adipose tissue (WAT) in C57BL/6J mice which were fed a regular or high-fat diet. Fourteen days following surgical castration profound effects on WAT tissue such as reductions in WAT wet weight and WAT/body weight ratio, induction of lipolysis and morphologic changes characterized by smaller adipocytes, and increased stromal cell compartment were documented in both dietary groups. Castrated animals had decreased serum leptin levels independent of diet but diet-dependent decreases in serum adiponectin and resistin. The castrated high-fat group had dramatically lower serum triglyceride levels. Immunohistochemical analysis revealed higher staining for smooth muscle actin, macrophage marker Mac-3, and Cxcl5 in the castrated than in the control mice in both dietary groups. We also detected increased fatty-acid synthase expression in the stromal compartment of WAT in the regular-diet group. Castration also reduces the expression of androgen receptor in WAT in the regular-diet group. We conclude that castration reduces tissue mass and affects biologic function of WAT in mice.

© 2011 Elsevier Ireland Ltd. All rights reserved.

1. Introduction

White adipose tissue (WAT) is a loose connective tissue that is crucial in the regulation of whole-body fatty-acid homeostasis. WAT is composed of adipocytes and other cells found in the stromal-vascular fraction, including macrophages, fibroblasts, pericytes, blood cells, endothelial cells, poorly differentiated mesenchymal cells, and preadipocytes (Fruhbeck, 2008). This dynamic, multifunctional endocrine tissue can secrete a large number of biologically active molecules, collectively called adipokines, which include hormones, growth factors, enzymes, cytokines, complement factors, and matrix proteins. For most of these molecules, WAT also expresses receptors that mediate extensive cross-talk both locally and systemically in response to specific external stimuli or metabolic changes (Fruhbeck, 2008; Galic et al., 2010). There is also an increasing body of evidence that a specific fat depot, the epididymal fat pad, produces a locally acting factor responsible for maintaining spermatogenesis in rodents (Chu et al., 2010; Hansel, 2010).

Storage of excessive fatty acids in an expanded adipose tissue mass characterizes obesity, which has reached epidemic proportions in the United States, where 35.1% of adults are now classified as obese (Catenacci et al., 2009). This epidemic is especially prob-

lematic because obesity is closely associated with the development of insulin resistance in peripheral tissues, such as skeletal muscle, and in the liver; moreover, it is an independent risk factor for the development of type 2 diabetes mellitus as well as myocardial infarction, stroke, and certain cancers (Galic et al., 2010). In fact, a high body mass index (BMI) is associated with increased risk of several common and less-common malignancies in a sex- and site-specific manner. An association has also been reported between obesity and metabolic syndrome and not only with increased risk for the development of cancer but also for the progression of certain types of cancer (Fair and Montgomery, 2009; Roberts et al., 2010).

Additionally, adipose tissue is a major site for inflammation because the visceral adipose tissue depot contains more macrophages and releases more inflammatory cytokines, such as monocyte chemoattractant protein 1 (MCP1)/CCL2, plasminogen activator inhibitor 1, and interleukin (IL) 6, IL-8, and IL-10, than subcutaneous adipose tissue does. In turn, inflammation in adipose tissue further increases the risk of obesity-related diseases and may be associated with the progression of cancer and its consequent mortality (Tran and Kahn, 2010).

The metabolism of adipose tissue is known to be affected by gonadal steroids such as testosterone. For example, testosterone deficiency, which can be caused by hypogonadism, aging, central obesity, or androgen-deprivation therapy in patients with prostate cancer, is associated with insulin resistance, type-2 diabetes, the metabolic syndrome, and cardiovascular disease in general (Bain, 2010).

* Corresponding author. Address: Department of Genitourinary Medical Oncology – Research, Unit 18-3, The University of Texas MD Anderson Cancer Center, 1515 Holcombe Boulevard, Houston, TX 77030-4009, USA. Tel.: +1 713 792 9955; fax: +1 713 792 9956.

E-mail address: timthomp@mdanderson.org (T.C. Thompson).

In mouse models, it has been demonstrated that cells from WAT are recruited by experimentally induced tumors and promote cancer progression (Zhang et al., 2009). Also, although surgical castration of mice results in increased glucose uptake into adipose tissue (Tran and Kahn, 2010), the effect of testosterone deficiency on adipose tissue has not been studied extensively.

Therefore, we undertook this study to identify the sustained effects of castration on WAT in adult male mice. We used C57BL/6J mice, which are commonly used for studies involving a high-fat diet (HFD) (Collins et al., 2004). We used a regular-diet and HFD approaches to assess differences in the responses to castration as the result of WAT deposition adjacent to the epididymis.

Our study results describe the changes in tissue mass, morphologic characteristics, induction of lipolysis, expression of genes coding for cytokines, and serum concentrations of adipokines that occurred in the epididymal WAT of adult mice fed a regular diet or a HFD after surgical castration.

2. Materials and methods

2.1. Animals and treatments

C57BL/6J mice, 5 and 10 weeks old, were purchased from MD Anderson Cancer Center's Department of Experimental Radiation Oncology. Mice were housed under specific pathogen-free conditions in facilities accredited by the American Association for Accreditation of Laboratory Animal Care, and all experiments were conducted in accordance with the principles and procedures outlined in the NIH's *Guide for the Care and Use of Laboratory Animals*.

For 7 weeks before and during the 2-week course of the experiments, the 5-week-old mice ($n = 45$) were fed a HFD (D12492; Research Diets, Inc., New Brunswick, NJ) containing 60 kcal% fat, 20 kcal% carbohydrate, and 20 kcal% protein, whereas the 10-week-old mice ($n = 30$) were fed a regular diet (Purina Conventional Rodent Chow 5001, St. Louis, MO) for 2 weeks. When all the mice were 12 weeks old, those in each dietary group were randomly allocated to three subgroups ($n = 10$ –15 mice each), one of which underwent sham surgery, and the other two, surgical castration. We analyzed two independent groups ($n = 30$ per group) of mice fed with a regular diet and combined data for further analysis.

For the surgeries, mice were anesthetized with 2–4% isoflurane. After the surgical site was shaved, an incision was made in the scrotum. In the sham-surgery group, the incision was then simply closed with sutures. For castration of the other two groups, the incision was made in the tunica of the first testicle, and the testis was pulled out and removed. The procedure was repeated on the contralateral side. The scrotal incisions were then closed with sutures. The sham-operated animals and half of the castrated ones then received a subcutaneously implanted empty pellet on their back, creating control and castrated + empty pellet (EP) groups, respectively. The second half of the castrated animals received implanted testosterone pellets, creating a castrated + testosterone pellet (TP) group. Both testosterone (25 mg testosterone, 21-days release time) and placebo pellets were purchased from Innovative Research of America (Sarasota, FL).

2.2. Blood and tissue sampling and processing

All mice from both dietary groups were euthanized by using the CO₂ inhalation method 2 weeks after having undergone the surgical and pellet-implantation procedures. Their body weight and length were recorded. Blood samples were collected from the posterior vena cava, allowed to clot overnight at 4 °C, and then centrifuged for 20 min at 2000g. The resulting serum was stored frozen at –80 °C.

Further, the epididymal WAT pads were collected from each mouse, as were the anterior, ventral, and dorsolateral lobes of the prostate, an androgen-dependent organ used as a control, and the wet weights of all those tissues were measured. WAT tissue was processed as follows: one half of WAT was snap-frozen in liquid nitrogen and stored at –80 °C for further analysis of protein expression and RNA extraction. The second half of WAT was fixed in paraformaldehyde, embedded in paraffin, and cut into 5- μ m sections for subsequent histologic and immunohistochemical (IHC) analyses.

2.3. Histological analysis of WAT

The effects of castration on the size of adipocytes were quantitatively evaluated using images, acquired at 20 \times magnification, of hematoxylin and eosin (H&E)-stained WAT sections. The analysis was performed with a Nikon Eclipse 90i image analysis system and the NIS-Elements AR software 3.0 (both from Nikon Instruments, Inc., Melville, NY). One hundred randomly selected adipocytes from each section were outlined using the manual function of the system, and the areas of individual adipocyte profiles were recorded. To analyze the size distribution of adipocytes, the histogram function in Excel (Microsoft Corporation, Redmont, WA) was used and graphs were created.

2.4. Western blotting

A portion of each WAT specimen was homogenized in ice-cold radioimmunoprecipitation assay buffer by using a battery-powered handheld homogenizer (Sigma–Aldrich, St. Louis, MO). The resulting suspension was then spun in a bench centrifuge at 16,000g for 10 min. The supernatant was collected and cleared by passage through a Vivaclear Mini clarifying filter (Sartorius Stedim Biotech, Aubagne, France). Protein concentration was measured by using a protein assay kit from Bio-Rad Laboratories (Hercules, CA). Conventional Western blotting was performed using the following primary antibodies to visualize proteins: hormone-sensitive lipase (Hsl), phospho-hormone-sensitive lipase (pHsl^{Ser660}), adipose triglyceride lipase (Atgl), and fatty acid synthase (Fasn) all from Cell Signaling Technology, Beverly, MA). Gapdh (Santa Cruz Biotechnology, Inc., Santa Cruz, CA) was used as a loading control. Images were quantified with UN-SCAN-IT gel software Version 6.1 (Silk Scientific, Inc., Orem, UT).

2.5. Enzyme-linked immunosorbent assay (ELISA)

Serum testosterone concentrations were measured by using an ELISA kit (Calbiotech, Spring Valley, CA) according to the manufacturer's instructions. Serum leptin, adiponectin, and resistin concentrations were measured by using an ELISA kit for a respective cytokine (R&D Systems, Inc., Minneapolis, MN) according to the manufacturer's instructions.

2.6. Measurement of serum glucose and triglyceride (TG) levels

Serum glucose levels were measured using a glucose (GO) assay kit (Sigma–Aldrich). The manufacturer's procedure was modified to minimize the use of serum: 1 μ l of serum was mixed with 99 μ l of distilled water, and 200 μ l of assay reagent was added. The reaction mix in a 1.7-ml test tube was incubated for 30 min at 37 °C. The reaction was stopped with 200 μ l of 6 M sulfuric acid, and then 100 μ l of the reaction mix was transferred to a 96-well plate. Absorbance at 540 nm was read by using a conventional plate reader.

Serum TG levels were measured by using a triglyceride assay kit (Cayman Chemical Company, Ann Arbor, MI) according to the manufacturer's protocol.

2.7. Gene-expression analysis

Total RNA was isolated from frozen WAT specimens by using a standard extraction protocol with Trizol reagent (Invitrogen Corporation, Carlsbad, CA). An iScript™ cDNA Synthesis Kit from Bio-Rad was used to generate cDNA for further analysis by quantitative real-time polymerase chain reaction (qRT-PCR) testing with SYBR Green stain. We initially used a Mouse Chemokines & Receptors RT² Profiler PCR Array (SA Biosciences, Frederick, MD) to detect genes that were affected by castration in epididymal WAT. Genes that were up-regulated after castration were further analyzed by using primers from PrimerBank (Spandidos et al., 2010).

2.8. IHC analysis

IHC with primary antibodies to the stromal marker smooth muscle α -actin (Acta2; 1:1000 dilution, Sigma, cat# A5228), Cxcl5 (1:50, R&D Systems, cat# MAB433), the macrophage marker Mac-3 (1:50, BD Biosciences, Pharmingen, San Diego, CA, cat# 550292), Fasn (1:50; Cell Signaling Technology, cat# 3180), and androgen receptor Ar (1:50, Santa Cruz Biotechnology, cat# sc-816) was performed on paraffin-embedded sections of WAT pads using the Vectastain® ABC kit or ImmPRESS™ reagents (Vector Laboratories, Inc., Burlingame, CA) according to the manufacturer's instructions. Specificity of the IHC staining was verified by incubating WAT sections with nonspecific rabbit or mouse immunoglobulin G in place of the primary antibody.

Acta2 and Fasn immunostaining was evaluated quantitatively using the Nikon Eclipse 90i with the NIS-Elements AR software. Fifteen to 20 images from each immunostained section of the WAT pad were randomly acquired at 10 \times magnification. The area of stroma that stained positively for Acta2 was detected by using a pixel classifier that recognizes brown DAB staining; the results were recorded as the percentage of the Acta2-positive stroma among a total tissue area.

To quantify the Cxcl5 and Mac-3 IHC staining results, we used the manual function to count the stromal cells that stained positively on 20 images acquired randomly at 20 \times magnification and recorded the total number of positively labeled cells for each antibody.

2.9. Statistical analysis

Statistical analysis was performed in Microsoft Office Excel using two-tailed Student's *t* testing. The level of significance was set at $p < 0.05$. Values are expressed as mean \pm SE.

3. Results

3.1. Castration induces changes in epididymal WAT

3.1.1. Regular-diet group

Analysis of epididymal WAT (20 mice in each group) wet weights revealed that in the castration + EP (castration) group of mice, the weight was lower than that in the sham-surgery control group (control) by 43% ($p < 0.001$), and in the castration + TP group, lower by 16% ($p = 0.01$) (Fig. 1A). The WAT wet weight/body weight ratios (Fig. 1B) were also lower, by 40% in the castration group and 22% in the castration + TP group, than in the control group ($p < 0.001$ for both comparisons). Together, these results indicate

that testosterone supplementation after surgical castration partially offsets the effect of castration.

As expected, castration resulted in significantly reduced wet weights of all prostatic lobes (Fig. 1S, Supplementary data). To detect changes in the size of adipocytes, we evaluated the H&E-stained WAT sections from five mice in each group. The adipocytes in the castration group appeared smaller than those in the control and castration + TP groups did (Fig. 1C). Indeed, quantitative image analysis (Fig. 1D) revealed that the average area of the adipocytes was less in the castration group ($1020 \pm 116 \mu\text{m}^2$; $p = 0.027$) than it was in the control ($1522 \pm 145 \mu\text{m}^2$) and the castration + TP ($1262 \pm 67 \mu\text{m}^2$) groups.

We also detected a change in the stroma that was characterized by more fibroblast-like stromal cells and macrophages in the WAT from the castrated group than there were in that from the control and castration + TP groups. Some small adipocytes were surrounded by stromal cells.

3.1.2. High-fat diet group

The HFD group had higher body weights, epididymal WAT wet weight/body weight ratios, and BMIs than the regular-diet group had (Fig. 2S, Supplementary data). The wet weights of the anterior, ventral, and dorsolateral prostate lobes, used as controls, are shown in Fig. 1S, Supplementary data.

Analysis of epididymal WAT (15 animals in each group) wet weight revealed that the castration group had reduced WAT wet weight by 53% ($p < 0.001$), and castration + TP group by 18% ($p = 0.3$) compared to the control group (Fig. 2A). The castration group had reduced WAT wet weight/body weight ratio by 47% ($p < 0.001$), and the castration + TP group by 16% ($p = 0.28$) compared to the control group (Fig. 2B).

The analysis of H&E-stained WAT sections revealed that the size of adipocytes was reduced in the castration group compared to the control group (Fig. 2C). Reduced size of adipocytes in the castrated group was confirmed by the quantitative image analysis (Fig. 2D). The average area of the adipocytes was $2555 \pm 257 \mu\text{m}^2$ after castration compared to $4166 \pm 228 \mu\text{m}^2$ in the control group. The presence of testosterone (i.e., castration + TP group) ($p = 0.003$) prevented the reduction of the size of adipocytes only partially as the adipocyte average area was $3388 \pm 268 \mu\text{m}^2$.

Thus, castration induces statistically significant WAT weight and the WAT wet weight/body weight ratio reduction independently of diet, but testosterone treatment partially offsets the effect of castration on WAT wet weight. Castration also induces morphologic changes in adipocytes: cells become smaller and have a larger stromal compartment. In general, castration led to reduced adipocyte size, and this effect was reversed in part by testosterone in the regular-fat diet group but not in the HFD group.

3.2. Castration-induced lipolysis

We hypothesized that castration induces lipolysis in WAT on the basis of our observations of reduced WAT wet weight and reduced size of adipocytes. To validate this hypothesis, we performed Western blotting to analyze protein levels of Hsl, pHsl^{Ser660}, and Atgl in WAT from both dietary groups after experimental treatments. Western blotting (Fig. 3) revealed reduced pHsl^{Ser660} levels by 46% ($n = 10$, $p = 0.004$) in WAT from the regular-diet group after castration. Atgl protein levels were reduced as well, but the reduction was not statistically significant. The protein level of Hsl was increased by 22% in the presence of testosterone; the pHsl^{Ser660} levels and Atgl levels were similar to those detected in the castration group but without statistical significance.

In contrast, we detected an increase of almost 2.5 times the pHsl^{Ser660} levels ($n = 5$, $p = 0.003$) and 40% increased Atgl protein levels ($n = 5$, $p = 0.006$) in WAT from the HFD group after

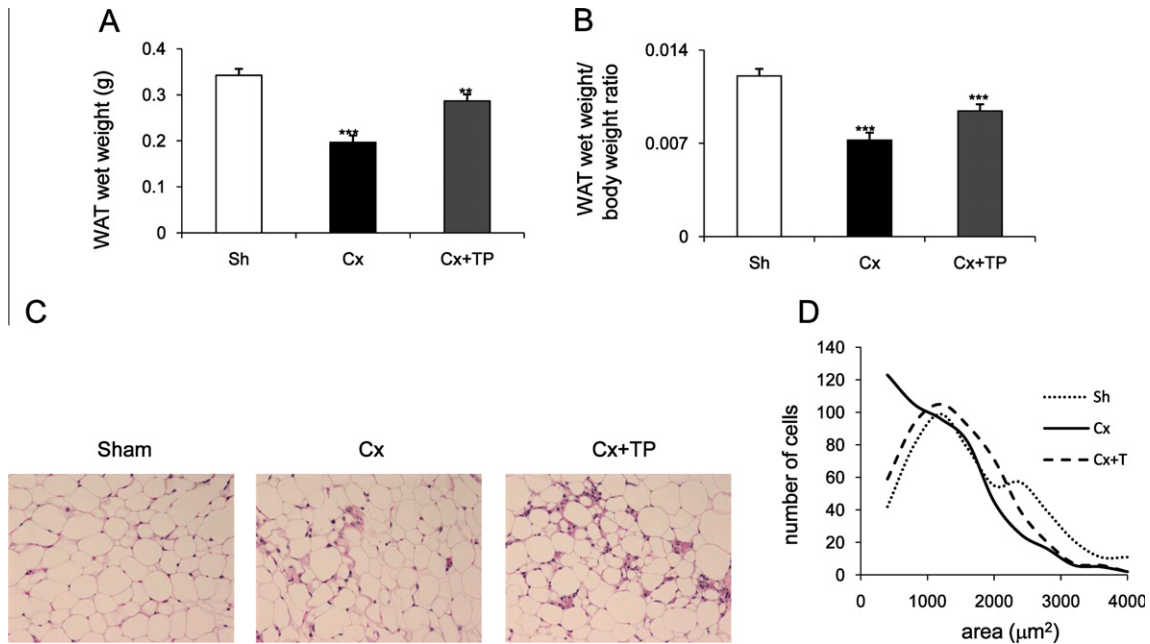


Fig. 1. The regular-diet group: (A) WAT wet weight, (B) WAT wet weight/body weight ratio, (C) hematoxylin and eosin staining of WAT, and (D) the adipocyte size distribution. (A) C57BL/6 mice fed regular diet were sham-operated, castrated, and castrated and treated with testosterone pellets as described in Section 2. At the end of the experiment, mice were euthanized and their WAT wet weights and body weights were recorded. Columns, WAT wet weight; bars, SE; ** $p < 0.01$; *** $p < 0.001$. (B) The WAT wet weight/body weight ratio was calculated. Columns, WAT wet weight/body weight ratio; bars, SE; *** $p < 0.001$. (C) Hematoxylin and eosin staining of WAT from sham-operated, castrated, and castrated + TP mice was performed as described in Section 2. Original magnification, 20 \times . (D) Line-graphs represent the adipocyte size distribution which was acquired by the image analyses. For each experimental group, 500 adipocytes were randomly selected from five specimens, and the areas of individual adipocytes were measured. Histogram function was used; bins were selected as 400 μm^2 increments.

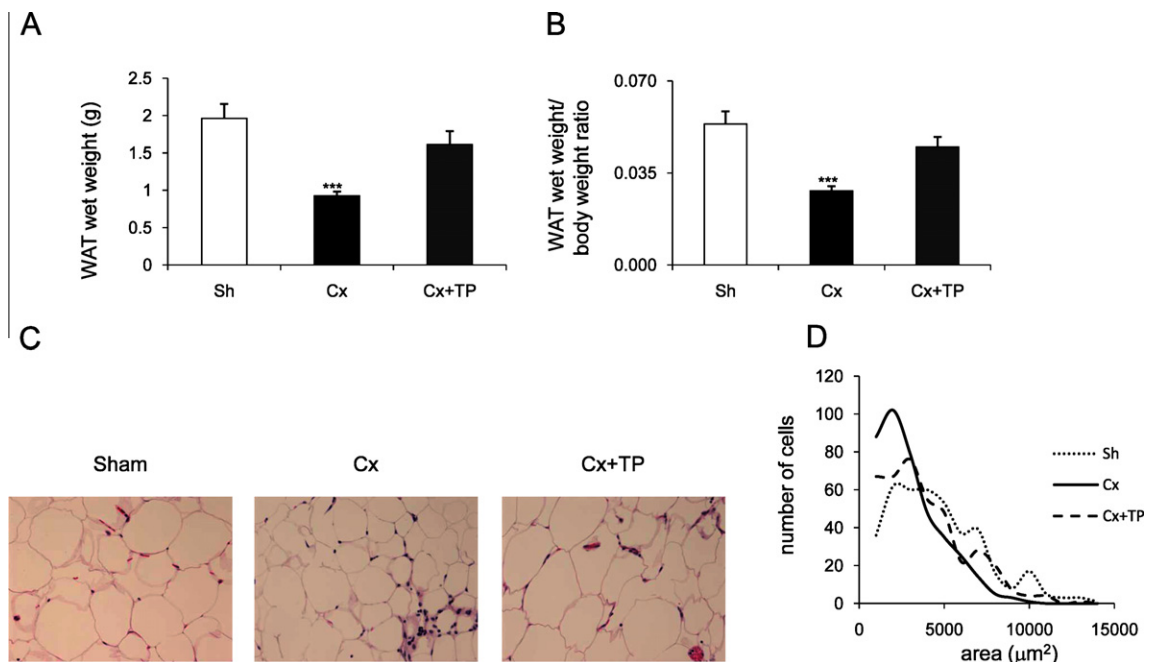


Fig. 2. The high-fat diet group: (A) WAT wet weight, (B) WAT wet weight/body weight ratio, (C) hematoxylin and eosin staining of WAT, and (D) the adipocyte size distribution. (A) C57BL/6 mice fed with high-fat diet were sham-operated, castrated, and castrated and treated with testosterone pellets as described in Section 2. At the end of the experiment, mice were euthanized and their WAT wet weights and body weights were recorded. Columns, WAT wet weight; bars, SE; ** $p < 0.01$; *** $p < 0.001$. (B) The WAT wet weight/body weight ratio was calculated. Columns, WAT wet weight/body weight ratio; bars, SE; *** $p < 0.001$. (C) Hematoxylin and eosin staining of WAT from sham-operated, castrated, and castrated + TP mice was performed as described in Section 2. Original magnification, 10 \times . (D) Line-graphs represent the adipocyte size distribution which was acquired by the image analyses. For each experimental group 500 adipocytes were randomly selected from five specimens and the areas of individual adipocytes were measured. Histogram function was used; bins were selected as 1000 μm^2 increments.

castration, suggesting that lipolysis is ongoing 14 days after castration. Differences detected in pHsl^{Ser660} and Atgl levels were offset by the presence of testosterone (Fig. 3).

Thus, it appears that castration-induced lipolysis in WAT of HFD-fed animals is more robust and/or sustained 14 days after castration than in animals fed a regular diet.

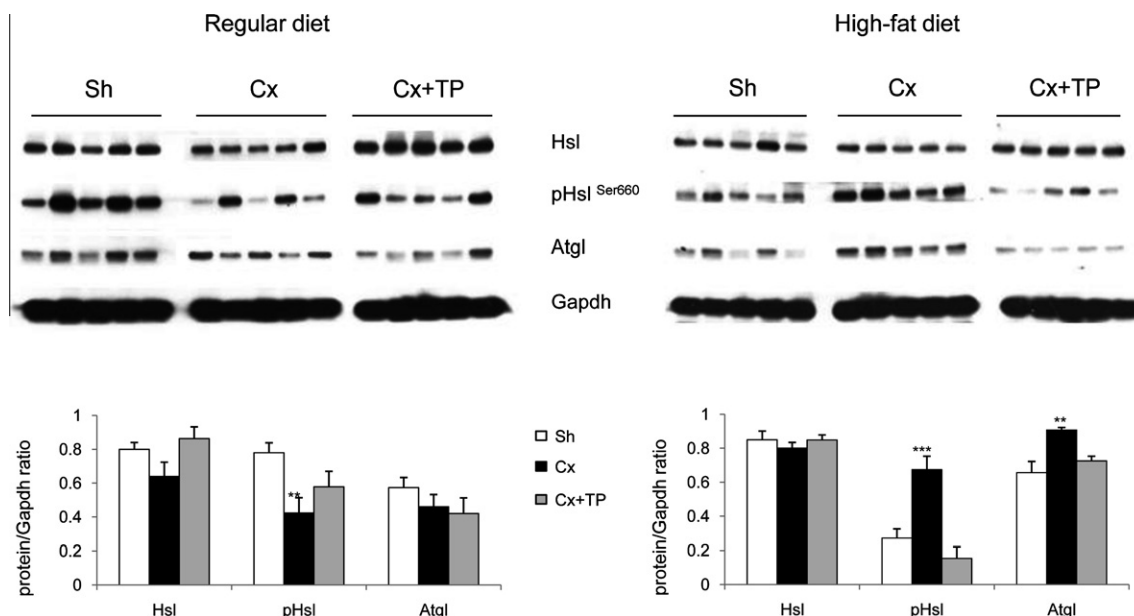


Fig. 3. Western blot analysis of hormone-sensitive lipase (Hsl), phosphorylated hormone sensitive lipase on serine 660 (pHsl^{Ser660}), adipose tissue triglyceride lipase (Atgl) protein levels in WAT from mice fed with regular diet and high-fat diet. Western blotting was performed as described in Section 2. Gapdh was used as a loading control. Images were quantified using UN-SCAN-IT gel 6.1 software to calculate protein/Gapdh ratio. Columns, protein/Gapdh ratio; bars, SE; ** $p < 0.01$; *** $p < 0.001$.

3.3. Serum adipokine levels

We further analyzed serum leptin, adiponectin, and resistin levels from mice from both dietary groups using commercial ELISA kits (Table 1). We detected reduced leptin levels in serum from the regular-diet group after castration by 72% ($n = 8$, $p < 0.001$) compared to the control group ($n = 8$). Castrated animals treated with TP also had reduced serum leptin levels by 46% ($n = 8$, $p = 0.007$) compared to the control group.

We detected increased adiponectin levels in serum from castrated mice by 13% ($n = 8$, $p = 0.0039$) compared to the control group. Castrated mice with TP had reduced serum adiponectin levels by 25% ($n = 8$, $p = 0.0004$) compared to the control group. Similarly, castration resulted in increased serum resistin levels by about 28% ($n = 8$, $p < 0.0001$) compared to the control group. Castrated mice with TP had serum resistin levels comparable with the control group.

The HFD group had reduced serum leptin levels after castration by 61% ($n = 8$, $p < 0.001$) compared to the control group ($n = 8$). Castrated animals treated with TP ($n = 8$) had serum leptin levels similar to the control group.

We did not detect castration-induced changes in serum adiponectin and resistin levels in castrated male mice compared to the controls.

Thus, mice fed a regular diet had reduced serum leptin and increased serum adiponectin and resistin levels after castration. The effect of testosterone was only partial as the serum leptin and adiponectin levels were lower compared to the control group. Castration had no effect on serum adiponectin and resistin levels in the HFD group.

3.4. Serum TG and glucose levels

We measured TG levels in serum collected from the control, castrated, and castrated + TP mice fed with a regular diet and HFD (Table 1). As expected, controls in the HFD group had higher serum TG levels than the controls in the regular-diet group had ($p = 0.03$). Castration of the regular-diet group resulted in a small but significant reduction in serum TG levels ($p = 0.018$) that was marginally offset by testosterone. However, castrated animals in the HFD group had three times lower serum TG levels than the control group had ($p = 0.002$). Castrated animals treated with testosterone had about two times lower serum TG levels than the control group had ($p = 0.013$), suggesting that testosterone did not offset the effect of castration.

We also measured serum glucose levels (Table 1). There were no differences in serum glucose levels in the regular-diet group. Control mice in the HFD group had significantly higher serum glu-

Table 1
Serum levels of adipokines, triglycerides (TG), and glucose.

	RD			HFD		
	Sh	Cx	Cx + TP	Sh	Cx	Cx + TP
Leptin (pg/ml)	2.5 ± 0.3	1.1 ± 0.2**	1.7 ± 0.3	24.3 ± 1.5	9.4 ± 0.9***	21.8 ± 2.0
Resistin (pg/ml)	22.4 ± 0.5	31.2 ± 1.1***	19.5 ± 1.0	30.6 ± 1.8	30.2 ± 2.2	28.7 ± 1.0
Adiponectin (μg/ml)	13.9 ± 0.1	15.6 ± 0.1**	10.4 ± 0.2***	13.6 ± 0.5	14.0 ± 0.3	12.9 ± 0.9
TG (mg/ml)	12.6 ± 0.8	10.4 ± 0.3*	11.2 ± 0.8	18.1 ± 2.5	6.3 ± 0.1**	9.3 ± 1.0*
Glucose (mg/ml)	2.3 ± 0.1	2.4 ± 0.1	2.4 ± 0.1	3.0 ± 0.1	3.6 ± 0.2*	3.4 ± 0.1*

Values are expressed as mean ± SE.

* $p < 0.05$.

** $p < 0.01$.

*** $p < 0.001$.

cose levels than the control mice from the regular-diet group had ($p = 0.004$). Castrated mice in the HFD group had increased serum glucose levels by 22% compared to the controls ($p = 0.027$). Increased serum glucose levels by about 14% were also detected in the castration + TP group compared to the controls ($p = 0.017$).

Thus, our data demonstrate that castration has a small but significant reduction of serum TG levels in the regular diet group and a dramatic reduction of serum TG in the HFD group. This effect was not offset by testosterone replacement in the HFD group. Serum glucose levels were affected only in the HFD group. Testosterone did not offset the castration effect.

3.5. Castration induces cytokines in epididymal WAT

It has been reported that in humans, visceral WAT generates and releases inflammatory cytokines, including CCL2, PAI-1, IL-6, IL-8, and IL-10, under specific conditions (Sengenès et al., 2007). We asked whether castration induces changes in the expression of genes coding for cytokines in epididymal WAT. qRT-PCR revealed that numerous cytokine genes are induced in WAT after castration. The most up-regulated genes were *Cxcl5*, *Cxcl2*, and *Il4* in WAT from the regular-diet group after castration (Table 2). Genes coding for *Cxcl5*, *Il1 α* , and *Mmp2* were the most up-regulated in WAT from the HFD group after castration (Table 3). We also detected reduced leptin mRNA after castration (Tables 2 and 3). In both dietary groups, mRNA levels of genes coding for cytokines were lower compared to controls after testosterone treatment (Tables 2 and 3). We also compared mRNA levels of cytokines in control mice from the regular-diet and HFD groups. We detected increased expression of genes coding for *Cxcl1* (59.3 ± 31.7), *Ccl7* (22.5 ± 4.3), *Ccl2* (15.5 ± 5.3), *Cxcl2* (12.3 ± 3.1), *Tnf* (11.8 ± 2.6), and *Ccl3* (10.0 ± 0.7) in the HFD group numbers in brackets are fold \pm SE.

Therefore, these experiments revealed that castration leads to changes in the expression of specific cytokine genes in epididymal WAT. *Cxcl5* was the most-induced cytokine in both dietary groups. Further, there is a set of cytokines which are produced at increased levels by WAT in the control HFD group compared to the control regular-diet group.

3.6. IHC staining of WAT

The H&E results suggested that castration induced morphologic changes in WAT associated with increased stromal compartment and macrophage infiltration (Figs. 1 and 2C). We performed IHC of paraffin-embedded WAT sections from the regular-diet

(Fig. 4A) and HFD (Fig. 4B) groups. We used Acta2 as a stromal marker and Mac-3 as a macrophage marker. We also labeled sections with *Cxcl5* and *Fasn* antibodies.

Fig. 4A shows stained sections and results of the quantitative analysis of WAT from mice on regular diet. Castration resulted in a significant increase of Acta2, Mac-3, and *Cxcl5* protein expression. Testosterone offset castration-induced increase of Mac-3 and *Cxcl5* proteins. *Cxcl5* staining pattern suggests that *Cxcl5* is most likely expressed by WAT macrophages.

We further hypothesized that increased presence of stromal cells in WAT is a result of the tissue regenerative process characterized by the presence of differentiating pre-adipocytes with the increased *Fasn* expression. IHC for *Fasn* confirmed that there is a subset of cells in WAT with increased *Fasn* staining. Increased *Fasn* staining was mostly localized to the stromal compartment of WAT after castration (Fig. 4A).

Fig. 4B shows stained sections and results of the quantitative analysis of WAT from the HFD group. Increased Acta2, Mac-3, and *Cxcl5* proteins were detected, although the increases did not reach the level of statistical significance. Testosterone offset the castration-induced increase of Mac-3 and *Cxcl5* proteins. We did not detect subset of WAT with increased *Fasn* staining in the HFD group (data not shown).

IHC staining for *Fasn* was confirmed by Western blotting (Fig. 3S, Supplementary data). We detected increased *Fasn* protein levels in WAT after castration in the regular-diet group compared to the control group (*Fasn*/*Gapdh* ratio was 1.15 vs 0.98, $n = 4$, $p = 0.008$). A slight increase of *Fasn* protein levels (*Fasn*/*Gapdh* ratio was 1.05 vs 0.98, $n = 4$) was not statistically significant in the castration + TP regular-diet group. We did not detect changes in *Fasn* protein levels in the HFD group.

Thus, IHC staining confirmed that castration-induced WAT morphologic changes are accompanied by changes in protein expression. We detected increased expression of Acta2, Mac-3, *Cxcl5*, and *Fasn*.

3.7. Effect of castration on the expression of androgen receptor *Ar* in WAT

Initially, we used ELISA to measure serum testosterone levels in samples ($n = 8$ per treatment group) from both diet groups. The analysis confirmed that castrated animals in both diet groups had background levels of serum testosterone; 0.04 ± 0.02 ng/ml or 0.05 ± 0.03 ng/ml in the regular-diet and the HFD group, respectively. We detected lower levels of serum testosterone in the control HFD group (0.26 ± 0.13 ng/ml; $p = 0.16$) than in the

Table 2
Changes in the cytokine expression in epididymal WAT 14 days after castration, regular diet.

Gene	Gene ID	Official name	Cx		Cx + TP	
			Fold	SE	Fold	SE
<i>Cxcl5</i>	20311	Chemokine (c-x-c motif) ligand 5	56.2	31.5	4.0	2.6
<i>Cxcl2</i>	20310	Chemokine (c-x-c motif) ligand 2	22.3	15.3	6.0	1.7
<i>Il4</i>	16189	Interleukin 4	15.9	7.6	4.1	2.4
<i>Ccl3</i>	20302	Chemokine (c-c motif) ligand 3	14.1	3.3	3.4	1.2
<i>Xcl1</i>	16963	Chemokine (c motif) ligand 1	9.7	5.2	1.7	0.0
<i>Il10</i>	16153	Interleukin 10	7.8	2.8	−1.2	1.3
<i>Ccl2</i>	20296	Chemokine (c-c motif) ligand 2	7.3	4.3	2.3	1.0
<i>Tnf</i>	21926	Tumor necrosis factor alpha	6.8	2.6	1.8	0.2
<i>Il1a</i>	16175	Interleukin 1 alpha	6.5	2.5	2.2	0.6
<i>Ccl4</i>	20303	Chemokine (c-c motif) ligand 4	6.3	1.4	−1.0	1.0
<i>Cxcl1</i>	14825	Chemokine (c-x-c motif) ligand 1	6.0	2.1	1.4	0.3
<i>Il6</i>	16193	Interleukin 6	5.5	1.6	1.8	0.4
<i>Ccl7</i>	20306	Chemokine (c-c motif) ligand 7	5.2	3.1	0.7	1.4
<i>Mmp2</i>	17390	Matrix metalloproteinase 2	4.3	0.5	2.1	0.5
<i>Tnfrsf1a</i>	21937	Tumor necrosis factor receptor superfamily, member 1a	3.1	0.5	1.6	0.4
<i>Lep</i>	16846	Leptin	−3.2	0.5	−0.1	1.2

Table 3

Changes in the cytokine expression in epididymal WAT 14 days after castration, high-fat diet.

Gene	Gene ID	Official name	Cx		Cx + TP	
			Fold	SE	Fold	SE
<i>Cxcl5</i>	20311	Chemokine (c-x-c motif) ligand 5	59.8	17.7	7.7	4.4
<i>Il1a</i>	16175	Interleukin 1 alpha	6.1	2.3	0.4	1.0
<i>Mmp2</i>	17390	Matrix metalloproteinase 2	6	0.8	1.0	1.3
<i>Il12</i>	16159	Interleukin 12	5.7	1.1	0.8	1.0
<i>Il4</i>	16189	Interleukin 4	5.4	1.6	−0.3	0.8
<i>Ccl3</i>	20302	Chemokine (c-c motif) ligand 3	4.8	1.6	3.7	1.1
<i>Il10</i>	16153	Interleukin 10	4.5	0.8	0.6	0.7
<i>Tnf</i>	21926	Tumor necrosis factor alpha	3.3	0.6	−0.1	0.8
<i>Ccl4</i>	20303	Chemokine (c-c motif) ligand 4	2.4	0.3	1.5	0.5
<i>Lep</i>	16846	Leptin	−4.4	1.7	−0.4	1.5

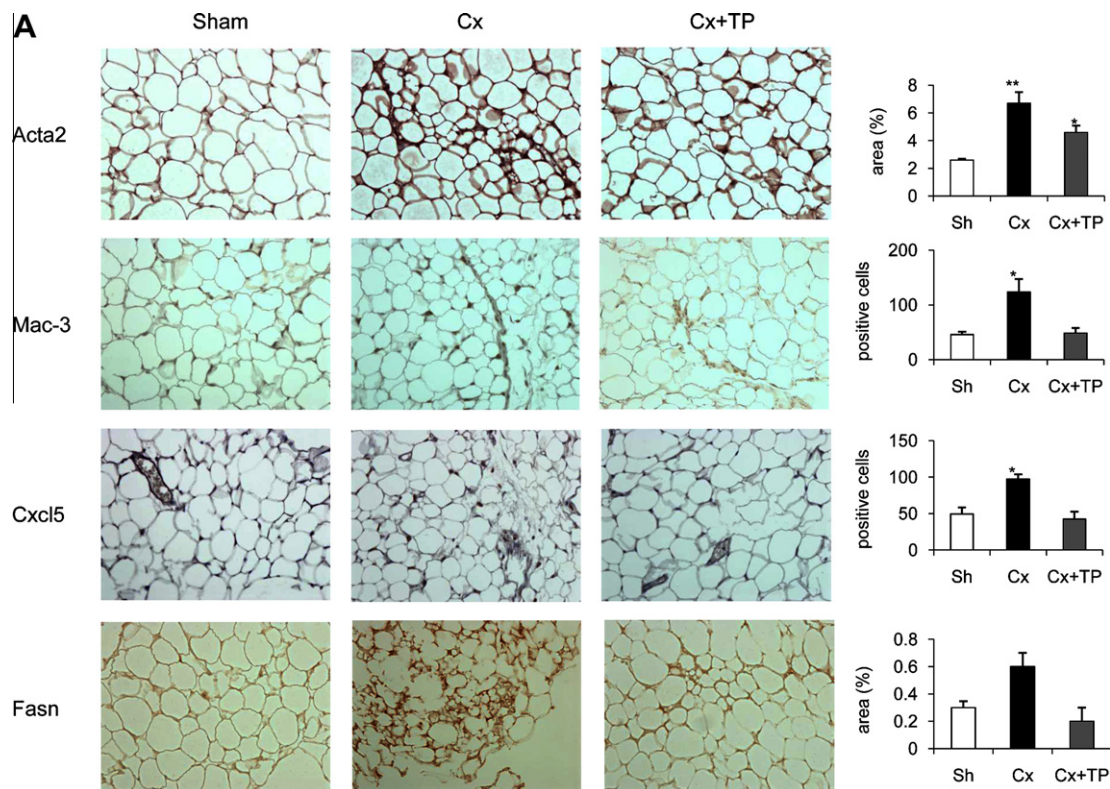


Fig. 4. Immunohistochemical (IHC) staining of paraffin-embedded WAT from mice fed a regular diet (A) or a high-fat diet (B). (A, B) Antibodies against smooth muscle actin (Acta2), Mac-3, Cxcl5, and Fasn were used as described in Section 2. Images were depicted at 20 \times magnification. Column graphs represent results from the semiquantitative analysis of the IHC images. Sh, sham-operated; Cx, castration; Cx + TP, castration + testosterone pellet. Bars, SE; * $p < 0.05$; ** $p < 0.01$.

regular-diet group (1.65 ± 0.57 ng/ml). Implantation of testosterone pellets resulted in serum testosterone levels of 23.63 ± 0.81 ng/ml or 17.59 ± 0.70 ng/ml in the regular-diet and the HFD castration + TP group, respectively.

To assess the effect of castration on the expression of Ar, we performed qRT-PCR and IHC staining of WAT sections from both diet groups. In the regular-diet group, castration resulted in reduced Ar mRNA by 4.1 ± 0.9 -fold. A similar decrease was detected in the castration + TP group (4.7 ± 1.4 -fold). IHC staining (Fig. 5) revealed that nuclear Ar was undetectable in WAT from the castrated regular-diet group. Fewer cells stained for nuclear Ar in WAT from the castration + TP group compared to the control group.

In WAT from the HFD group, the Ar mRNA and protein levels are very low to undetectable (data now shown).

Thus, castration results in the reduced expression of Ar in WAT on both mRNA and protein levels. Ar mRNA and protein is not detectable in WAT from animals fed HFD.

4. Discussion

Our data demonstrate that surgical castration has profound effects on WAT. The WAT wet weight and the WAT wet weight/body weight ratio were lower in the castration + TP group and reached statistical significance in the regular-diet group. These results suggest that testosterone does not fully abrogate effects of castration in the regular-diet group. Morphologic changes after castration were associated with adipocyte size reduction, an increase in a stromal compartment, and macrophage infiltration.

Our data further indicate that lipolytic enzymes can be activated in a sustained fashion in response to castration, as observed in the HFD group. We also detected increased Atgl protein levels in the HFD group after castration. Our data further indicate that animals in the HFD group respond differently to the castration stimulus than animals in the regular-diet group, potentially as a consequence of a more robust and/or sustained lipolytic program.

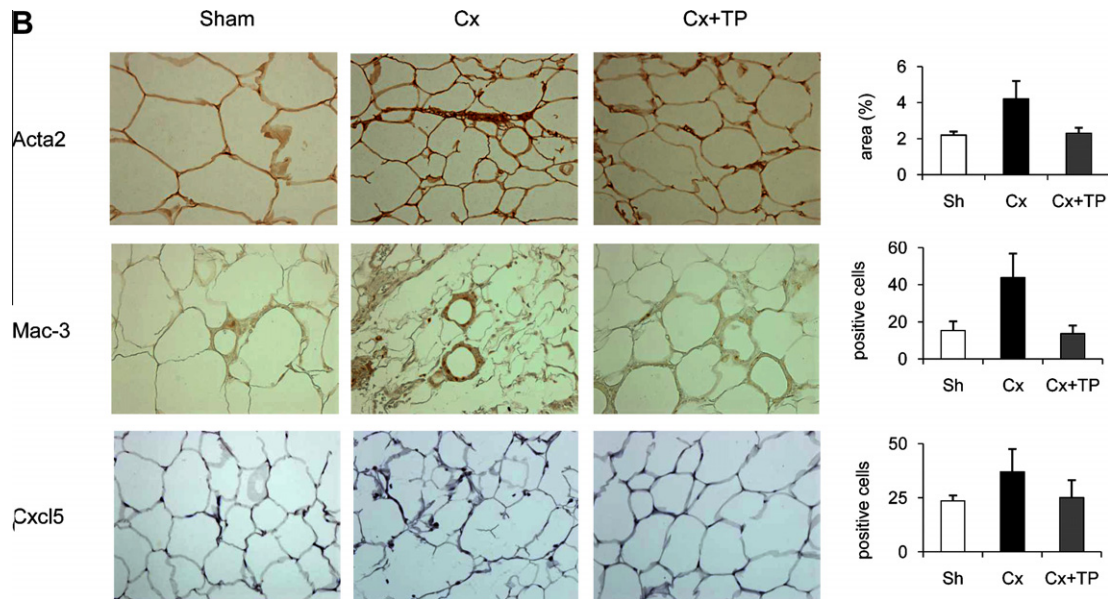


Fig. 4 (continued)

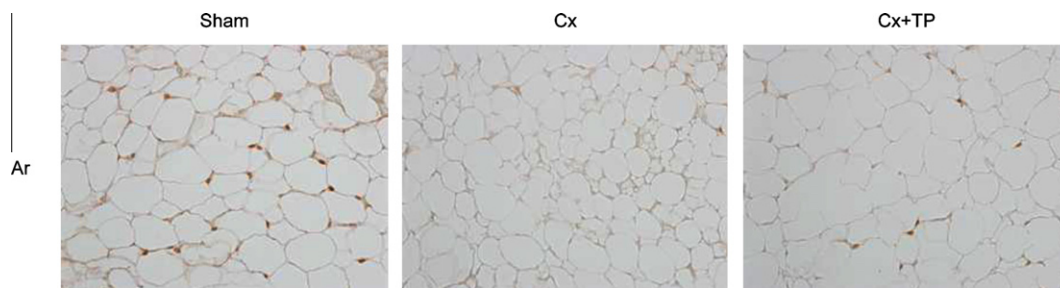


Fig. 5. Immunohistochemical staining for androgen receptor (Ar) of paraffin-embedded WAT from mice fed a regular diet. Antibodies against Ar were used as described in Section 2. Images were depicted at 20× magnification. Sh, sham-operated; Cx, castration; Cx + TP, castration + testosterone pellet.

In our view, these data further suggest that the lipolytic process does not continue indefinitely and may subside at a certain set-point. It may take longer for the HFD group to reach such set-point as lipolysis is still ongoing 14 days after castration. Future studies that analyze pHs^{Ser660} and Atgl protein levels at different time points after castration under various conditions may clarify this hypothesis.

Serum leptin levels were reduced in both dietary groups after castration, whereas serum resistin and adiponectin levels were increased in the regular-diet group after castration. Serum resistin and adiponectin levels were not affected by castration in the HFD group. Inoue et al. (2010) reported increased plasma adiponectin levels in castrated C57BL/6 mice independent of diet, and decreased plasma leptin levels in castrated mice on high carbohydrate diet. Xu et al. (2005) measured increased serum adiponectin levels in castrated C57BL/6 mice.

Controls in the HFD group had higher body weight, the WAT wet weight/body weight ratio and BMI than the controls in regular-diet group at the time of sacrifice (Fig. 2S, Supplementary data). We also measured serum glucose and triglyceride (TG) levels. Our data demonstrate that castration has a small but significant effect in the regular diet group and a profound effect on serum TG levels in the HFD group. This effect was modified but not offset by testosterone replacement. Serum glucose levels were also affected only in the HFD group by castration and testosterone did not offset the castration effect. Our results suggest that castration alters the

mechanism(s) regulating serum TG and glucose levels, selectively in the HFD group. The physiological mechanisms responsible for these metabolic changes need further investigation.

In addition to leptin, adiponectin, and resistin, adipose tissue expresses a wide range of factors, including pro-inflammatory cytokines and chemokines. The expression of IL-8, MCP-1/CCL2, and macrophage inflammatory protein is increased with adiposity in animals and humans (Sengenès et al., 2007). We detected *Cxcl5*, *Cxcl2*, and *Il4* in the regular-diet group and *Cxcl5*, *Il1a*, and *Mmp2* in the high-fat-diet group among the most induced cytokines after castration. The mRNA levels of *Cxcl1*, *Ccl7*, *Ccl2*, *Cxcl2*, *Tnf*, and *Ccl3* were higher in the control WAT from the HFD group than they were in the control regular-diet group. Chemokines and their corresponding receptors, including CCL2, CCL5, CXCL5, CXCL13, CXCL16, and CXCR5, have been shown to be involved in prostate cancer progression and organ-specific metastasis (Loberg et al., 2006; Sung et al., 2008; Singh et al., 2009). Further studies are needed to characterize cytokine-producing cells types in WAT.

We hypothesized that increased presence of stromal cells may be a result of the tissue regeneration process induced in WAT by castration. We detected increased Fasn staining in the stromal compartment of WAT from castrated mice, suggesting that the stromal compartment is involved in WAT remodeling after castration. Fasn is highly expressed in differentiating mouse 3T3-L1 pre-adipocytes (Paulauskis and Sul, 1988).

Interestingly, few cells within the stromal compartment in WAT from the castration + TP regular-diet group stained for Fasn. This suggests that testosterone may inhibit differentiation of stromal pre-adipocytes. It was reported that testosterone inhibits adipogenic differentiation of mouse 3T3-L1 pre-adipocytes (Singh et al., 2006).

It has been suggested that macrophages present in non inflamed tissue (i.e., resident macrophages) help maintain homeostasis and participate in tissue remodeling. In mice, these cells originate from circulating CCR2⁺CX3CR1^{hi} monocytes. In contrast, CCR2⁺CX3CR1^{low} monocytes migrate into inflamed tissue and differentiate into macrophages, which coordinate inflammatory responses by producing chemokines and clearing debris by phagocytosis (Lumeng et al., 2007). Future studies may explain the origin and provide an expression profile of macrophages that are found in WAT after castration.

Dieudonne et al. (1998) documented that human and rat pre-adipocytes and adipocytes express androgen receptor and suggested that androgens may contribute, through regulation of their own receptors, to the control of adipose tissue development. Yu et al. (2008) generated adipose-specific Ar knockout mice by a conditional genetic knockout approach. Dhindsa et al. (2010) reported that obesity is probably the condition most frequently associated with subnormal free testosterone concentrations in males. Our analysis confirmed the expression of Ar in epididymal WAT from mice fed regular diet and that the consumption of high-fat diet may result in the reduction of the Ar expression and reduced serum testosterone levels. Kyprianou and Isaacs, (1988) demonstrated that castration induced a series of temporally discrete biochemical events, including rapid loss of nuclear Ar and programmed cell death, within the rat ventral prostate. We detected the loss of nuclear Ar in WAT after castration but no apparent apoptosis (data not shown). Thus, mechanisms leading to reduced Ar levels at the time points analyzed in WAT after castration ought to be further studied.

Complex short-term effects of castration in rodents have not been studied in great detail. Published studies focus on long-term effects of castration (Koncarevic et al., 2010; Axell et al., 2006; Hastings and Hill, 1997; Vanderschueren et al., 2004) which are relevant to men undergoing androgen deprivation therapy. We hypothesize that we fortuitously selected a time point at which biochemical events which contribute to the effects of long-term androgen deprivation therapy in WAT are initiated.

In conclusion, our study demonstrated that castration has profound effects on mouse epididymal WAT. Future studies involving human WAT are needed to understand underlying biologic mechanisms during castration and to test the clinical relevance of these findings to the management of obesity, metabolic syndrome, and prostate cancer in humans.

Grants

This research is supported in part by the NIH grant R01CA050588, the DOD grant PC093932, and in part by the NIH through MD Anderson's Cancer Center Support Grant, CA016672.

Conflict of interest statement

None of the authors have any conflict of interest to declare.

Acknowledgements

The authors thank Karen F. Phillips, ELS, from the Department of Genitourinary Medical Oncology, MD Anderson Cancer Center, for editorial assistance.

Appendix A. Supplementary data

Supplementary data associated with this article can be found, in the online version, at doi:10.1016/j.mce.2011.07.011.

References

- Axell, A.M., MacLean, H.E., Plant, D.R., Harcourt, L.J., Davis, J.A., Jimenez, M., Handelsman, D.J., Lynch, G.S., Zajac, J.D., 2006. Continuous testosterone administration prevents skeletal muscle atrophy and enhances resistance to fatigue in orchidectomized male mice. *Am. J. Physiol. Endocrinol. Metab.* 291, E506–E516.
- Bain, J., 2010. Testosterone and the aging male: to treat or not to treat? *Maturitas* 66, 16–22.
- Catenacci, V.A., Hill, J.O., Wyatt, H.R., 2009. The obesity epidemic. *Clin. Chest. Med.* 30, 415–444, vii.
- Chu, Y., Huddleston, G.G., Clancy, A.N., Harris, R.B., Bartness, T.J., 2010. Epididymal fat is necessary for spermatogenesis, but not testosterone production or copulatory behavior. *Endocrinology* 151, 5669–5679.
- Collins, S., Martin, T.L., Surwit, R.S., Robidoux, J., 2004. Genetic vulnerability to diet-induced obesity in the C57BL/6J mouse: physiological and molecular characteristics. *Physiol. Behav.* 81, 243–248.
- Dhindsa, S., Miller, M.G., McWhirter, C.L., Mager, D.E., Ghanim, H., Chaudhuri, A., Dandona, P., 2010. Testosterone concentrations in diabetic and nondiabetic obese men. *Diabetes Care* 33, 1186–1192.
- Dieudonne, M.N., Pecquary, R., Boumediene, A., Leneuve, M.C., Giudicelli, Y., 1998. Androgen receptors in human preadipocytes and adipocytes: regional specificities and regulation by sex steroids. *Am. J. Physiol.* 274, C1645–52.
- Fair, A.M., Montgomery, K., 2009. Energy balance, physical activity, and cancer risk. *Methods Mol. Biol.* 472, 57–88.
- Fruhbeck, G., 2008. Overview of adipose tissue and its role in obesity and metabolic disorders. *Methods Mol. Biol.* 456, 1–22.
- Galic, S., Oakhill, J.S., Steinberg, G.R., 2010. Adipose tissue as an endocrine organ. *Mol. Cell Endocrinol.* 316, 129–139.
- Hansel, W., 2010. The essentiality of the epididymal fat pad for spermatogenesis. *Endocrinology* 151, 5565–5567.
- Hastings, I.M., Hill, W.G., 1997. The effect of testosterone in mice divergently selected on fat content or body weight. *Genet. Res.* 70, 135–141.
- Inoue, T., Zakikhani, M., David, S., Algire, C., Blouin, M.J., Pollak, M., 2010. Effects of castration on insulin levels and glucose tolerance in the mouse differ from those in man. *Prostate* 70, 1628–1635.
- Koncarevic, A., Cornwall-Brady, M., Pullen, A., Davies, M., Sako, D., Liu, J., Kumar, R., Tomkinson, K., Baker, T., Umiker, B., Monnell, T., Grinberg, A.V., Liharska, K., Underwood, K.W., Ucran, J.A., Howard, E., Barberio, J., Spaitis, M., Pearsall, S., Seehra, J., Lachey, J., 2010. A soluble activin receptor type IIb prevents the effects of androgen deprivation on body composition and bone health. *Endocrinology* 151, 4289–4300.
- Kyprianou, N., Isaacs, J.T., 1988. Activation of programmed cell death in the rat ventral prostate after castration. *Endocrinology* 122, 552–562.
- Loberg, R.D., Day, L.L., Harwood, J., Ying, C., St John, L.N., Giles, R., Neeley, C.K., Pienta, K.J., 2006. CCL2 is a potent regulator of prostate cancer cell migration and proliferation. *Neoplasia* 8, 578–586.
- Lumeng, C.N., Deyoung, S.M., Bodzin, J.L., Saltiel, A.R., 2007. Increased inflammatory properties of adipose tissue macrophages recruited during diet-induced obesity. *Diabetes* 56, 16–23.
- Paulauskis, J.D., Sul, H.S., 1988. Cloning and expression of mouse fatty acid synthase and other specific mRNAs: developmental and hormonal regulation in 3T3-L1 cells. *J. Biol. Chem.* 263, 7049–7054.
- Roberts, D.L., Dive, C., Renehan, A.G., 2010. Biological mechanisms linking obesity and cancer risk: new perspectives. *Annu. Rev. Med.* 61, 301–316.
- Sengenès, C., Miranville, A., Lolmede, K., Curat, C.A., Bouloumie, A., 2007. The role of endothelial cells in inflamed adipose tissue. *J. Intern. Med.* 262, 415–421.
- Singh, R., Artaza, J.N., Taylor, W.E., Braga, M., Yuan, X., Gonzalez-Cadavid, N.F., Bhasin, S., 2006. Testosterone inhibits adipogenic differentiation in 3T3-L1 cells: nuclear translocation of androgen receptor complex with beta-catenin and T-cell factor 4 may bypass canonical Wnt signaling to down-regulate adipogenic transcription factors. *Endocrinology* 147, 141–154.
- Singh, S., Singh, R., Sharma, P.K., Singh, U.P., Rai, S.N., Chung, L.W., Cooper, C.R., Novakovic, K.R., Grizzle, W.E., Lillard Jr., J.W., 2009. Serum CXCL13 positively correlates with prostatic disease, prostate-specific antigen and mediates prostate cancer cell invasion, integrin clustering and cell adhesion. *Cancer Lett.* 283, 29–35.
- Spandidos, A., Wang, X., Wang, H., Seed, B., 2010. PrimerBank: a resource of human and mouse PCR primer pairs for gene expression detection and quantification. *Nucleic Acids Res.* 38, D792–9.
- Sung, S.Y., Hsieh, C.L., Law, A., Zhou, H.E., Pathak, S., Multani, A.S., Lim, S., Coleman, I.M., Wu, L.C., Figg, W.D., Dahut, W.L., Nelson, P., Lee, J.K., Amin, M.B., Lyles, R., Johnstone, P.A., Marshall, F.F., Chung, L.W., 2008. Coevolution of prostate cancer and bone stroma in three-dimensional coculture: implications for cancer growth and metastasis. *Cancer Res.* 68, 9996–10003.
- Tran, T.T., Kahn, C.R., 2010. Transplantation of adipose tissue and stem cells: role in metabolism and disease. *Nat. Rev. Endocrinol.* 6, 195–213.
- Vanderschueren, D., Vandenput, L., Boonen, S., Lindberg, M.K., Bouillon, R., Ohlsson, C., 2004. Androgens and bone. *Endocr. Rev.* 25, 389–425.

- Xu, A., Chan, K.W., Hoo, R.L., Wang, Y., Tan, K.C., Zhang, J., Chen, B., Lam, M.C., Tse, C., Cooper, G.J., Lam, K.S., 2005. Testosterone selectively reduces the high molecular weight form of adiponectin by inhibiting its secretion from adipocytes. *J. Biol. Chem.* 280, 18073–18080.
- Yu, I.C., Lin, H.Y., Liu, N.C., Wang, R.S., Sparks, J.D., Yeh, S., Chang, C., 2008. Hyperleptinemia without obesity in male mice lacking androgen receptor in adipose tissue. *Endocrinology* 149, 2361–2368.
- Zhang, Y., Daquinag, A., Traktuev, D.O., Amaya-Manzanares, F., Simmons, P.J., March, K.L., Pasqualini, R., Arap, W., Kolonin, M.G., 2009. White adipose tissue cells are recruited by experimental tumors and promote cancer progression in mouse models. *Cancer Res.* 69, 5259–5266.